Thiol-Triggered Deconstruction of Bifunctional Silyl Ether Terpolymers via an S_NAr-Triggered Cascade

Christopher M. Brown,[a] Keith E. L. Husted,[a] Yuyan Wang,[a] Landon J. Kilgallon,[a] Peyton Shieh,[a] Hadiqa Zafar,[a] David J. Lundberg [a,b] and Jeremiah A. Johnson[a,c*]

[a] Department of Chemistry, Massachusetts Institute of Technology, 77 Massachusetts Avenue, Cambridge, MA 02139, USA

[b] Department of Chemical Engineering, Massachusetts Institute of Technology, 77 Massachusetts Avenue, Cambridge, MA 02139, USA

[c] David H. Koch Institute for Integrative Cancer Research, Massachusetts Institute of Technology, 77 Massachusetts Avenue, Cambridge, Massachusetts 02139, USA

Abstract

While Si-containing polymers can often be deconstructed using chemical triggers such as fluoride, strong acids, and bases, they are resistant to cleavage by mild reagents such as biological nucleophiles, thus limiting their end-of-life options and potential environmental degradability. Here, using ring-opening metathesis polymerization, we synthesize terpolymers of (1) a "functional" monomer (e.g., a polyethylene glycol macromonomer or dicyclopentadiene); (2) a monomer containing an electrophilic pentafluorophenyl (PFP) substituent; and (3) a cleavable monomer based on a bifunctional silyl ether ($SiR_2(OR'_2)$). Exposing these polymers to thiols under basic conditions triggers a cascade of nucleophilic aromatic substitution (S_NAr) at the PFP groups, which liberates fluoride ions, followed by cleavage of the backbone Si–O bonds, inducing polymer deconstruction. This mild, thiol-triggered method is shown to be effective for deconstruction of PEGylated graft terpolymers in organic or aqueous conditions as well as polydicyclopentadiene (pDCPD)-based thermosets, significantly expanding upon the versatility of bifunctional silyl ether based functional polymers.

Introduction

Polymers that undergo selective bond cleavage[1] in response to an external trigger have numerous applications, including in drug delivery,[2–4] sensing,[5,6] transient electronics,[7,8] and recyclable materials.[9,10] A wide range of functional groups (e.g., azo,[11–13] dihydrofuran,[14] disulfide,[15,16] diselenium,[17] ester,[18] ketal,[19] poly(benzyl ethers),[20] phosphoramidate[21]) have been employed to enable triggered polymer deconstruction, and various external stimuli such as redox,[22,23] pH,[24,25] light,[12] heat,[26] nucleophiles,[27] and mechanical force[28] have been extensively studied. Nevertheless, there is often a trade-off between the introduction of cleavable bonds and polymer stability under use conditions, especially when mild cleavage reagents (e.g., biological triggers), and thus easier-to-cleave bonds, are required.

Bifunctional silyl ethers ($SiR_2(OR'_2)$; "BSEs") are versatile functional groups that have found applications as fluoride- and acid/base-cleavable linkages in, for example, biomaterials,[29] controlled release systems,[30–32] and deconstructable thermosets (Fig. 1A).[33–37] BSEs offer a unique combination of synthetic accessibility, compositional diversity,[38] and excellent thermal and oxidative stabilities while providing for highly selective cleavage with rates that can be easily controlled through variation of the Si–R substituents.[39] Moreover, cyclic olefins containing BSEs are suitable monomers for the synthesis of deconstructable homopolymers,[40] copolymers,[39] and industrial thermosets via ring-opening metathesis polymerization.[35–38,41] Nevertheless, while acid and/or fluoride are convenient triggers for BSE cleavage, there are instances where such stimuli are not compatible with a desired application, leading us to consider alternative methods.

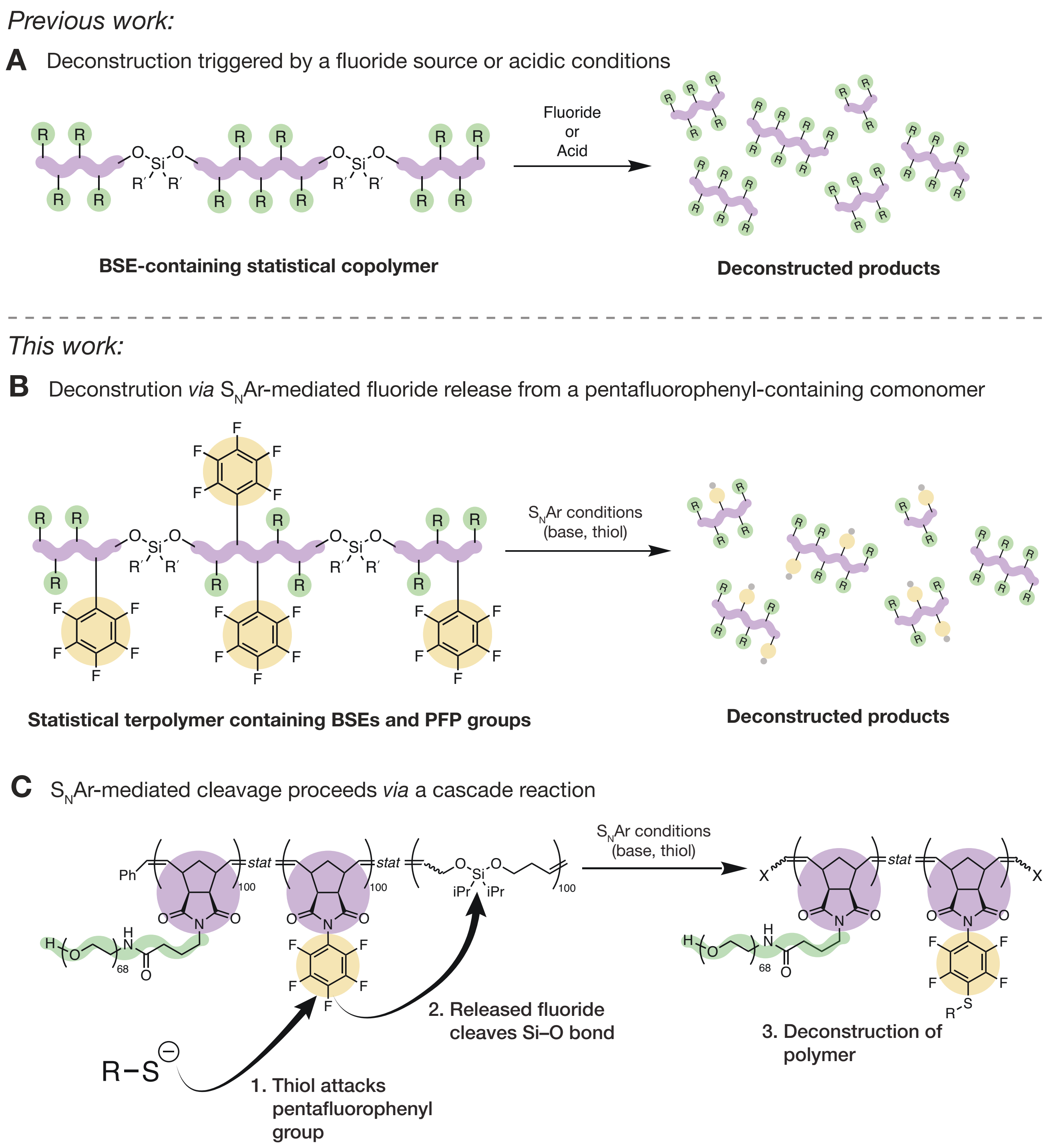

Fig. 1. (A) We have previously reported degradable materials containing bifunctional silyl ethers (BSEs) where polymer degradation is initiated by a fluoride source (e.g., tetrabutylammonium fluoride, TBAF) or acidic conditions (e.g., HCl). Cleavage of the silyl ether leads to degradation of the terpolymer backbone, resulting in the production of degradation fragments. (B) Here, we describe a class of polymeric materials containing pentafluorophenyl (PFP) comonomers which triggers decomposition upon exposure to nucleophilic aromatic substitution (S_NAr) conditions (a thiol in the presence of base). (C) The S_NAr-mediated cleavage proceeds via a cascade reaction. The produced thiolate attacks at the *para*-position of the PFP ring *via* S_NAr, releasing a fluoride ion, which in turn cleaves the Si–O bond of the BSE.

Inspired by advances in radical ring-opening polymerization—where sensitive electrophilic functional groups such as thioesters can be installed within polymer backbones to enable cleavage via nucleophilic attack[27,42,43]—and with interest in biodegradable polymers, we sought a strategy to facilitate the deconstruction of BSE-based polymers prepared via ROMP through exposure to nucleophiles such as thiols. While BSEs are not sufficiently reactive to undergo cleavage in the presence of thiols under typical conditions, we hypothesized that is would be possible to embed latent, thiolate-triggered fluoride sources into BSE-containing polymers to facilitate Si–O bond cleavage following a nucleophilic aromatic substitution (S_NAr) event. S_NAr reactions of pentafluorophenyl (PFP) derivatives[44] using a range of nucleophiles (e.g., alcohols,[45] amines,[46] phosphites,[47] thiols[44,48,49]) liberate one equivalent of F^- per substitution reaction, which we imagined could be utilized as the first step in an S_NAr, fluoride release, and BSE cleavage cascade (Fig. 1B). Additionally, S_NAr reactions of PFP groups are known to be effective reactions for polymer functionalization.[50–54] PFPs are compatible with ROMP, and there are many cheap, benign, and/or biologically-derived thiols that could potentially be used to initiate such a cascade process. Here, we present the realization of this concept, showing that linear, bottlebrush, and covalently crosslinked thermoset terpolymers with BSE and PFP containing monomers undergo selective backbone cleavage via a thiol-triggered S_NAr cascade. This work provides a new strategy to enable backbone cleavage of otherwise highly stable polymeric materials and extends the scope of BSE-based cleavage reactions for responsive materials design.[1]

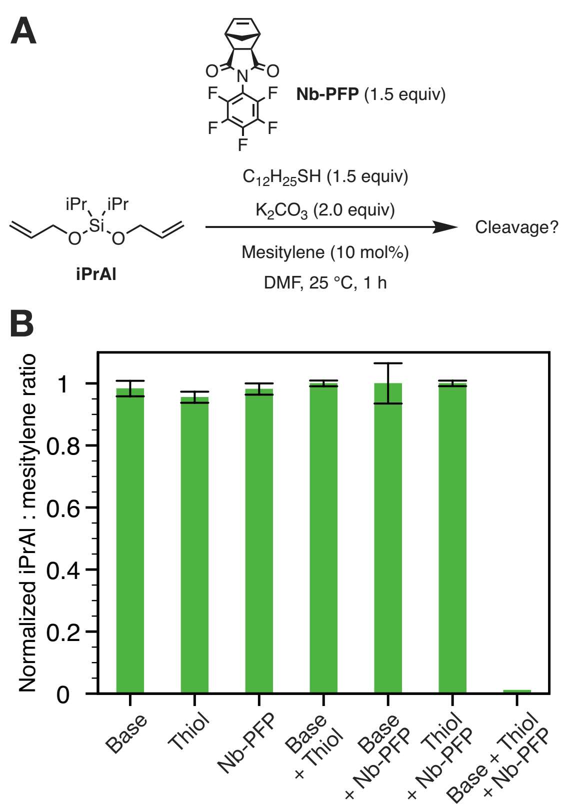

Fig. 2. (A) Scheme showing the methodology for the small molecule GC-MS studies of acyclic analogue **iPrAl**. (B) Bar chart comparing the ratio of **iPrAl** to a mesitylene internal standard (10 mol%) from GC-MS runs. **iPrAl** is reacted with either K_2CO_3

(base), **Nb-PFP**, 1-dodecanethiol (thiol), or combinations of the above in DMF for 1 h at 25 °C. Ratios calculated using peak integration and averaged over three runs. Error bars show standard deviation.

Results and Discussion

Small molecule model studies

First, we sought to determine whether or not BSEs are stable under typical conditions used for S_NAr reactions involving PFP groups, which often involve polar organic solvents and bases such as K_2CO_3, Cs_2CO_3 or 1,8-diazabicyclo[5,4,0]undec-7-ene (DBU).[44] PFP-based monomer **Nb-PFP** (synthesized following a reported procedure[55]) and **iPrAl**, a BSE mimic of a polymer backbone, were exposed to various conditions relevant to S_NAr (Fig. 2A); gas chromatography-mass spectrometry (GC-MS) was used to monitor **iPrAl** degradation/cleavage (mesitylene was used as an internal standard; see Supplementary Information section "Small Molecule GC-MS Studies" for further information; see Supplementary Information section "Small Molecule Syntheses" for details). Notably, **iPrAl** remains intact when treated with either 1-dodecanethiol (nucleophile, 1.5 equiv), K_2CO_3 (base, 2.0 equiv), **Nb-PFP** (latent fluoride, 1.5 equiv), a combination of 1-dodecanethiol and K_2CO_3 (nucleophile and base only), or with a combination of **Nb-PFP** and K_2CO_3 (latent fluoride and base) (Fig. 2B). When **iPrAl** was exposed to 1-dodecanethiol (1.5 equiv), K_2CO_3 (2.0 equiv), and **Nb-PFP** (1.5 equiv, i.e., all three reagents critical for S_NAr), however, >98% cleavage was observed after 1 h and no trace of **iPrAl** was seen after 2 h (Fig. S1). ^{19}F NMR spectroscopy of the reaction mixture showed a doublet of doublets of doublets and a multiplet with a downfield shift when compared to the parent **Nb-PFP** (Fig. S2A). This spectrum agrees well with the spectrum obtained for an independently synthesized, authentic sample of the expected *para*-1-dodecanethiol-substituted product **Nb-PFP-$SC_{12}H_{25}$** (see Supplementary Information section "Small Molecule Syntheses" for details). Moreover, a ^{19}F–^{19}F COSY experiment showed a correlation between the two new ^{19}F resonances generated under the reaction conditions (Fig. S2B). Altogether, these results confirm that S_NAr occurs between 1-dodecanethiol and **Nb-PFP** in the presence of K_2CO_3, and that the resulting fluoride can cleave a model BSE.

Nb-PFP homopolymer model studies

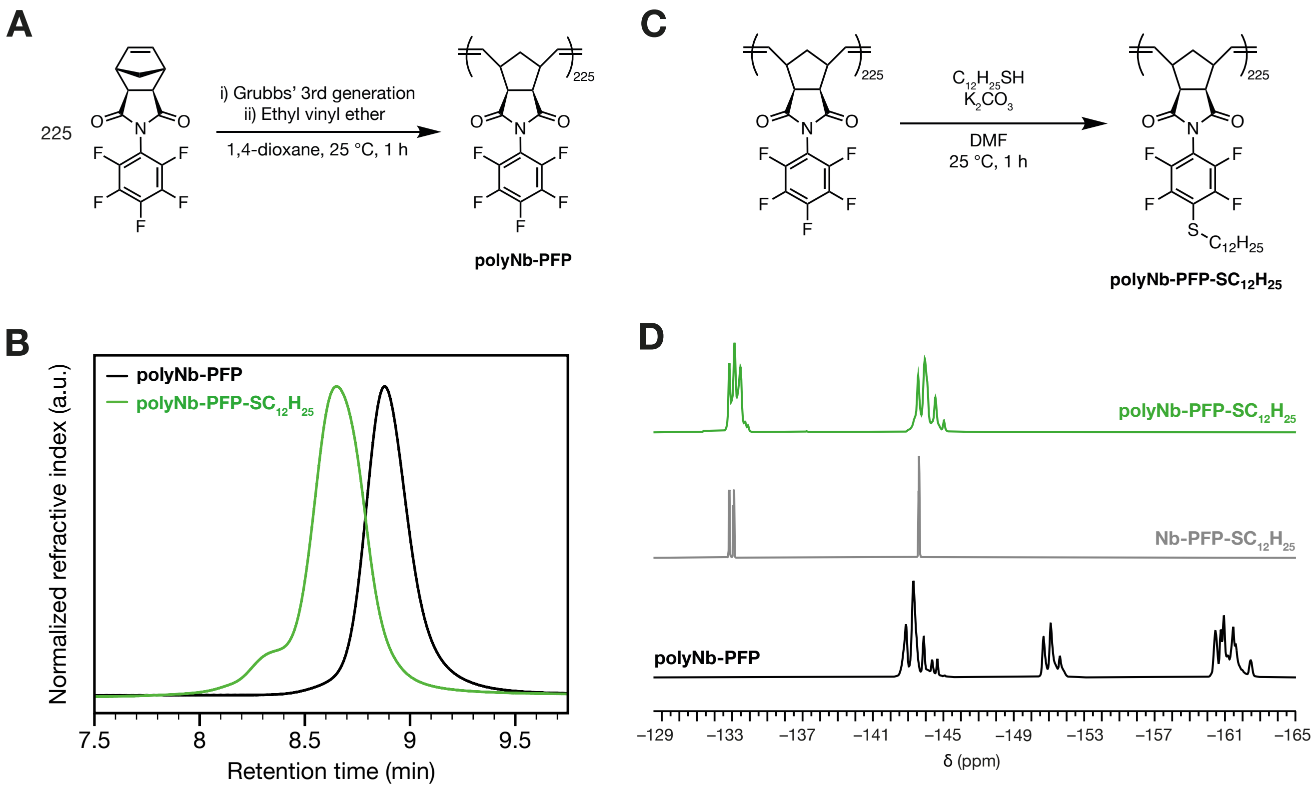

Fig. 3 (A) Synthesis of **polyNb-PFP** homopolymer. (B) SEC traces ($CHCl_3$ mobile phase) of **polyNb-PFP** (black) and S_NAr product **polyNb-PFP–SC$_{12}$H$_{25}$**. (C) Synthesis of S_NAr product **polyNb-PFP-SC$_{12}$H$_{25}$**. (D) ^{19}F NMR spectra (565 MHz, $CDCl_3$, 25 °C) comparing polyNb-PFP (black) to monomer **Nb-PFP–SC$_{12}$H$_{25}$** (grey) **and polyNb-PFP–SC$_{12}$H$_{25}$** (green).

To test the viability of S_NAr on a PFP-containing polymeric system, we subjected **Nb-PFP** (225 equiv) to ring-opening metathesis polymerization (ROMP) using Grubbs' 3rd generation bispyridyl initiator (1 equiv) in 1,4-dioxane, providing **polyNb-PFP** (Fig. 3A, see Supplementary Information section "Polymer Syntheses" for details). The ^{1}H NMR spectrum of **polyNb-PFP** agrees well with that reported by Tlenkopatchev and coworkers for similar polymers synthesized using Grubbs 1st and 2nd-generation initiators.[56] Complete consumption of **Nb-PFP** was observed (Fig. S3). ^{19}F NMR showed the same three general sets of resonances for **polyNb-PFP** and **Nb-PFP** (Fig. S4). **PolyNb-PFP** had a low dispersity ($Đ$ = 1.05) and a number average molecular weight (M_n) of 78,400, close to its theoretical M_n of 74,100, as determined by size exclusion chromatography (SEC, $CHCl_3$ mobile phase) (Fig. 3B, black trace). Exposure of **polyNb-PFP** to $C_{12}H_{25}SH$ (1.2 equiv) and K_2CO_3 (2.0 equiv) in DMF at 25 °C (Fig. 3C, see Supplementary Information section "Polymer Syntheses" for details) for 1 h gave quantitative conversion to the *para*-substituted S_NAr product as determined by ^{19}F NMR spectroscopy (Fig. 3D). SEC ($CHCl_3$ mobile phase) showed a concomitant increase in molecular weight (M_n of 123,800, close to its theoretical M_n of 115,100) and slight increase in dispersity ($Đ$ = 1.15) as determined by an earlier retention time (Fig. 3B). A small shoulder is observed, which we attribute to aggregation of the substituted polymer, likely caused by the addition of dodecyl groups along the main polymer chain.

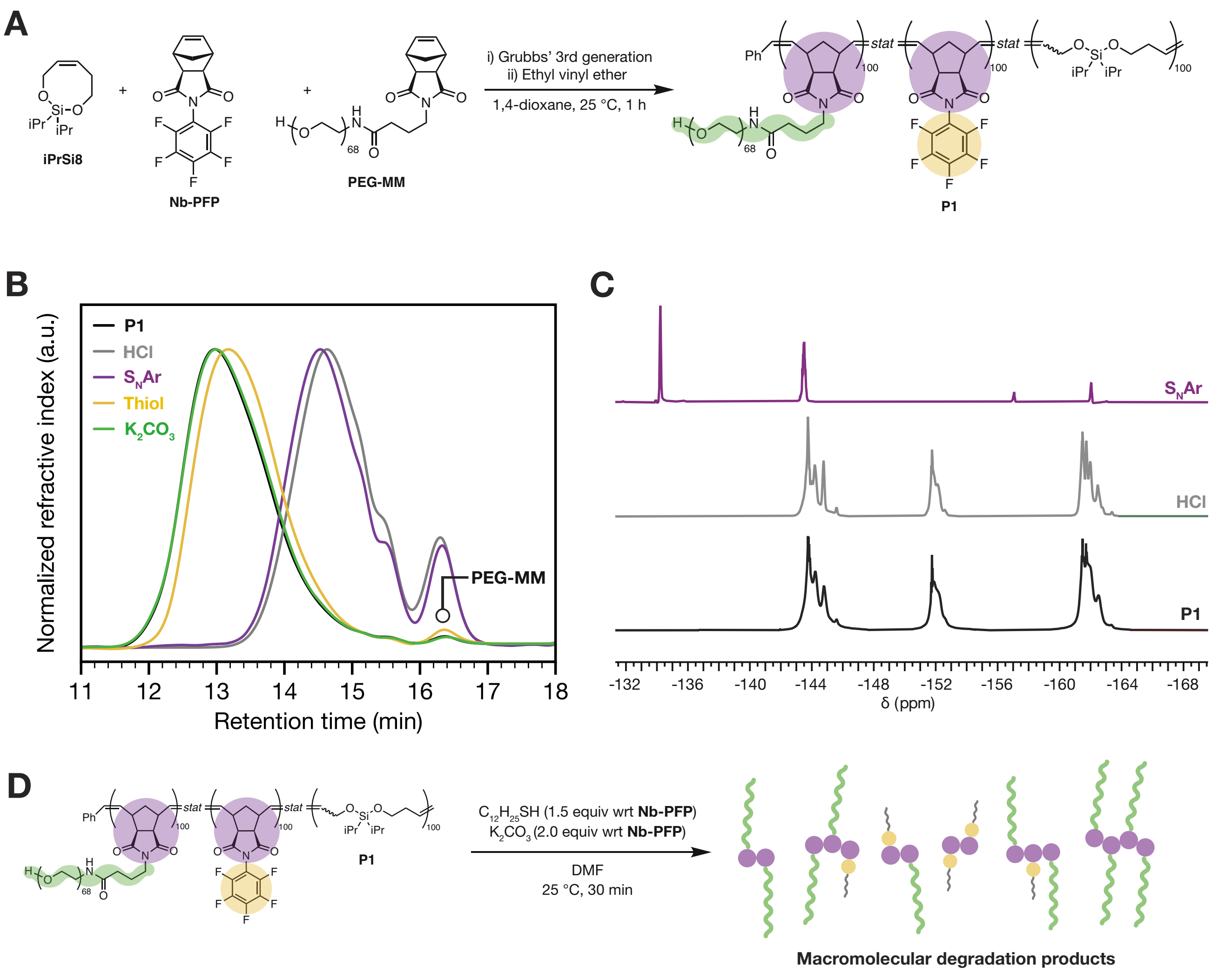

Fig. 4. (A) Synthesis of polynorbornene bottlebrush polymer **P1** *via* ROMP. Incorporation of **PEG-MM** into the terpolymer enables facile tracking of the degradation. (B) SEC traces (DMF mobile phase) showing polymer **P1** (black), the control degradation of **P1** using HCl (grey), the control degradation of **P1** using K_2CO_3 (green), the control degradation of **P1** using 1-dodecanethiol (thiol, yellow) and the degradation of **P1** using the S_NAr conditions of 1-dodecanethiol and K_2CO_3 (purple). (C) ^{19}F NMR spectra (565 MHz, $CDCl_3$, 25 °C) comparing the parent terpolymer **P1** (black), to the degradation products using HCl (grey), or S_NAr conditions (purple). (D) Schematic showing the degradation of **P1** using S_NAr conditions.

Terpolymer deconstruction using an S_NAr-initiated cascade.

After successfully demonstrating S_NAr of **polyNb-PFP**, we set out to test our hypothesis that an S_NAr-triggered cascade can enable deconstruction of polymers with backbone BSE groups. **Nb-PFP** was combined with BSE-containing monomer **iPrSi8** (synthesized according to a reported procedure[39]) and norbornene-terminated 3 kDa polyethylene glycol (PEG) macromonomer[57] **PEG-MM** in a 1:1:1 molar ratio in 1,4-dioxane and exposed to Grubbs' 3rd-generation bis-pyridyl initiator to generate graft terpolymer **P1** (total monomer:initiator ratio 300:1) (Fig. 4A, see Supplementary Information section "Polymer Syntheses" for experimental details). High conversions of **iPrSi8**, **Nb-PFP** and **PEG-MM** were confirmed via ^{1}H NMR (Fig. S5) and ^{19}F NMR spectroscopy (Fig. S6) to yield **P1** with M_n of 636,000 (±18.6%) and $Đ$ = 1.57 (See Supplementary Information section "Materials and Methods" for a discussion on M_n calculations and dn/dc value used). To confirm that BSEs are incorporated into the polymer backbone, **P1** was exposed to 1 M aqueous HCl (see Supplementary Information section "Degradation Studies" for experimental details), conditions previously shown to cleave BSEs in norbornene-based terpolymers.[39] SEC analysis revealed macromolecular deconstruction products at longer retention times, indicative of polymer backbone cleavage resulting in monomers, dimers, trimers, and higher oligomers[39] (Fig. 4B). Moreover, ^{19}F NMR spectroscopy shows that the PFP group remains unaffected under these conditions (Fig. 4C).

Gratifyingly, exposure of **P1** to S_NAr conditions—K_2CO_3 (2.0 equiv w.r.t. **Nb-PFP** in the terpolymer) and 1-dodecanethiol (1.5 equiv w.r.t. **Nb-PFP** in the terpolymer) in DMF—for 30 min at 25 °C led to backbone deconstruction and a nearly identical SEC trace to that for HCl-induced deconstruction (Fig. 4B, purple trace; see Supplementary Information section "Degradation Studies" for experimental details). ^{19}F NMR spectroscopy confirms formation of the expected S_NAr product, suggesting that deconstruction is triggered by S_NAr (Fig. 4C). Notably, exposing the polymer to K_2CO_3 alone (in DMF at room temperature) for the same time period does not lead to any polymer cleavage by SEC (Fig. 4B, green trace, M_n = 536,000 (±17.1%), $Đ$ = 1.53); exposing the polymer to 1-dodacenethiol in the absence of base leads to a small shift in the SEC peak to longer retention time, suggesting a small amount of decomposition likely due to background S_NAr (Fig. 4B, yellow trace, M_n = 268,000 (±14.6%), $Đ$ = 1.57).

PEG-based graft terpolymer deconstruction under aqueous conditions

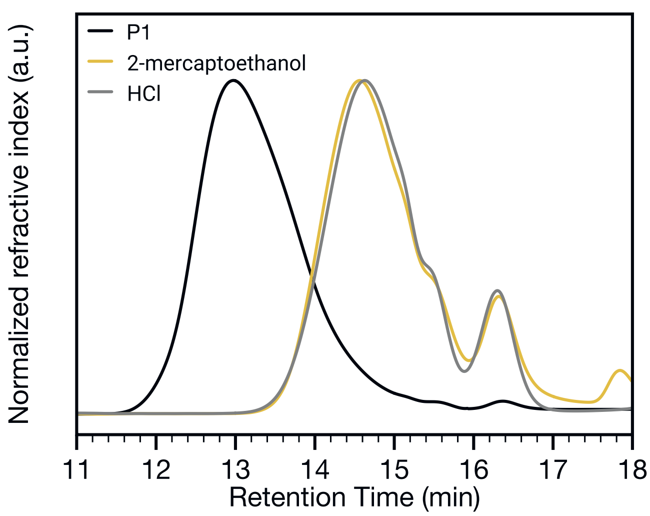

Fig. 5. Degradation of **P1** in pH 12 buffer. SEC traces (DMF mobile phase) of the parent terpolymer (black), HCl degraded material (grey), and **P1** reacted with 2-mercaptoethanol in pH 12 Na_2HPO_4/NaOH buffer solution (yellow).

We initially designed **iPrSi8** and related monomers[39] for the purpose of enabling the deconstruction of PEG-based graft terpolymers under aqueous conditions that may be translatable to applications in drug delivery and biological imaging.[58–62] Delaittre and coworkers reported thiol-mediated S_NAr of PFP-containing poly(*N*,*N*-dimethylacrylamide) in alkaline water (pH ≥ 11),[63] which inspired us to investigate backbone deconstruction of **P1** under similar conditions. First, we exposed the polymer to Na_2HPO_4/NaOH buffer solution (pH = 12; see Supporting Information section "Degradation Studies" for full experimental details) for 30 min at 25 °C; very little change was observed by SEC following this treatment, suggesting that the polymer is stable in aqueous alkaline buffer (Fig. S7). When 2-mercaptoethanol (1.5 equiv per PFP group) was added to this solution, which is sufficiently basic to generate the corresponding thiolate (pK_a of 2-mercaptoethanol = 9.72),[64] complete polymer deconstruction was observed in 30 min at room temperature (Fig. 5). ^{19}F NMR spectroscopy confirms the formation of S_NAr products, consistent with S_NAr-induced fluoride release and BSE cleavage (Fig. S8).The efficiency of this reaction is notable; previous work suggested that elevated temperatures (e.g., 40 °C), extend reaction times (e.g., 72 h), and large excesses of thiols (e.g., 10–20 equiv) are needed to induce S_NAr of polymeric PFP groups under aqueous conditions.[63] Here, deconstruction may be facilitated by the hydrophobic local environment of **P1**, where the PFP and BSE groups reside, which may elevate the local concentration of thiol and/or stabilize the S_NAr transition state.

Thiol-triggered cascade deconstruction of polydicyclopentadiene thermoset

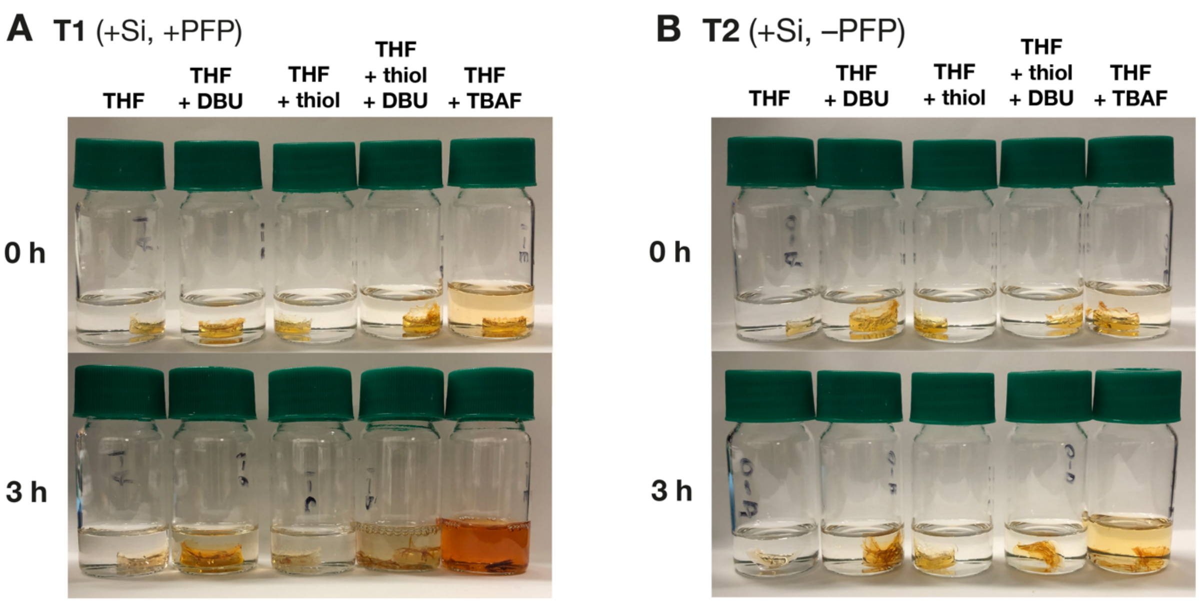

Fig. 6. Degradation of doped pDCPD thermoset materials. (A) Thermoset **T1** (+Si, +PFP) containing pDCPD, **iPrSi8** (10% v/v) and **Nb-PFP** (2.0 equiv w.r.t. **iPrSi8**) in solutions of: THF; THF and DBU; THF and 1-dodecanethiol (thiol); THF, thiol, and DBU; THF and TBAF at 25 °C, after 0 and 3 h. (B) Thermoset **T2** (+Si, –PFP) containing pDCPD and **iPrSi8** (10% v/v) in solutions of: THF; THF and DBU; THF and 1-dodecanethiol (thiol); THF, thiol, and DBU; THF and TBAF at 25 °C, after 0 and 3 h.

We have shown that BSE-containing monomers such as **iPrSi8** can be copolymerized with dicyclopentadiene (DCPD) to generate deconstructable[38,41] and remoldable[35] polydicyclopentadiene (pDCPD) thermosets and composites, offering a new end-of-life strategy for this high-performance engineering material.[65] Nevertheless, in these studies we have used 1M TBAF, 1M HCl, or high-temperature treatment with octanoic acid as deconstruction triggers; we hypothesized that our S_NAr-triggered cascade process could serve as an alternative method for pDCPD deconstruction.

To test this hypothesis, we prepared two thermosets: the first—thermoset **T1** (Fig. 6A)—was prepared by curing a liquid resin containing DCPD (14.4 equiv) with 10% v/v of **iPrSi8** (1.0 equiv) and **Nb-PFP** (2.0 equiv); the second—thermoset **T2** (Fig. 6B)—was prepared by curing a resin containing DCPD with 10% v/v of **iPrSi8** only (see Supporting Information section "Thermoset Materials" for full experimental details). Two equivalents of **Nb-PFP** w.r.t. **iPrSi8** were chosen to facilitate full material deconstruction; as there are 2 Si–O bonds per BSE, 2 equiv of fluoride are required to achieve complete Si–O bond cleavage. Dynamic mechanical analysis (DMA, Fig. S9, Table S1) showed that the glass transition temperature (T_g) of **T1** (T_g = 67 °C) was depressed compared to **T2** (T_g = 134 °C); however, thermogravimetric analysis (TGA, Fig. S10, Table S2) showed that the decomposition temperatures (T_d) of **T1** (T_d = 458 °C (plus a secondary shoulder at 550 °C due to addition of **Nb-PFP**)) and **T2** (T_d = 464 °C) were similar, suggesting that the addition of **Nb-PFP** does not have a major negative impact on the stability of these two thermoset materials. The storage moduli (E') and loss moduli (E'') of the thermosets were determined by DMA (Figs. S11 and S12, respectively). **T1** and **T2** displayed similar E' at 30 °C when compared to a neat pDCPD sample. Lower rubbery moduli were observed for **Nb-PFP**-containing **T1** when compared to **T2** or neat pDCPD, which is consistent with a reduced crosslink density due to dilution with **Nb-PFP** comonmer.[35]

Both thermosets were exposed to S_NAr conditions,[44] in this case using 1-dodecanethiol (2.0 equiv w.r.t. PFP groups) and the organic base 1,8-diazabicyclo[5,4,0]undec-7-ene (DBU, 2.0 equiv) in tetrahydrofuran (THF) solvent, which facilitates swelling of the crosslinked materials. In line with our hypothesis, **T1** was almost completely deconstructed (8% residual mass) to form soluble products under these conditions (Fig. 6A) while **T2** remained intact (Fig. 6B). Both thermosets were dissolved in 1M TBAF in THF (4% residual mass), confirming that the stability of **T2** under S_NAr conditions is due to a lack of latent fluoride groups. Moreover, **T1** did not dissolve in the presence of 1-dodecanthiol or DBU alone (Figs. S13–16). ^{19}F NMR analysis of the soluble fragments of **T1** deconstruction showed that under TBAF conditions (Fig. S17), the three sets of resonances corresponding to the PFP group are retained and additional ^{19}F resonances consistent with difluorosilane cleavage products are observed,[36] in line with direct cleavage of the Si–O bond by TBAF. By contrast, fragments from S_NAr conditions show two downfield ^{19}F resonances (Fig. S18), which is consistent with S_NAr of the PFP groups.

Conclusions

In summary, we describe a new method to deconstruct BSE-containing macromolecules using thiol-mediated S_NAr of PFP groups, which liberates fluoride and induces Si–O bond cleavage. The method is shown to be applicable to soluble graft terpolymers and insoluble thermosets, and it works in organic (DMF and THF) solvents or water with appropriate base (K_2CO_3, DBU, and phosphate buffer) and nucleophile (1-dodecanethiol and 2-mercaptoethanol). This approach expands the scope of BSE chemistry and may provide new ways to couple chemical triggers (e.g., thiols) with polymer deconstruction to achieve novel functions and end-of-life options.

Notes

CMB, PS and JAJ are named inventors on a patent application (US Provisional Application No. 63/195,259) filed by the Massachusetts Institute of Technology on the monomers and copolymers in this work.

Acknowledgements

This work was supported by the NSF Center for the Chemistry of Molecularly Optimized Networks (MONET, CHE-2116298). We thank Dr. Mohanraja Kumar for assistance with GC-MS studies. CMB acknowledges the Natural Sciences and Engineering Research Council of Canada (NSERC) for a Postdoctoral Fellowship. PS acknowledges the American Cancer Society for a Postdoctoral Fellowship and DJL acknowledges support from the National Science Foundation (NSF) Graduate Research Fellowship Program.

References

(1) Shieh, P.; Hill, M. R.; Zhang, W.; Kristufek, S. L.; Johnson, J. A. Clip Chemistry: Diverse (Bio)(Macro)Molecular and Material Function through Breaking Covalent Bonds. *Chem. Rev.* **2021**, *121* (12), 7059–7121. https://doi.org/10.1021/acs.chemrev.0c01282.

(2) Kamaly, N.; Yameen, B.; Wu, J.; Farokhzad, O. C. Degradable Controlled-Release Polymers and Polymeric Nanoparticles: Mechanisms of Controlling Drug Release. *Chem. Rev.* **2016**, *116* (4), 2602–2663. https://doi.org/10.1021/acs.chemrev.5b00346.

(3) Sharma, P.; Negi, P.; Mahindroo, N. Recent Advances in Polymeric Drug Delivery Carrier Systems. *Adv. Polym. Biomed. Appl.* **2018**, 369–388.

(4) Bawa, K. K.; Oh, J. K. Stimulus-Responsive Degradable Polylactide-Based Block Copolymer Nanoassemblies for Controlled/Enhanced Drug Delivery. *Mol. Pharm.* **2017**, *14* (8), 2460–2474. https://doi.org/10.1021/acs.molpharmaceut.7b00284.

(5) Hosseini, E. S.; Dervin, S.; Ganguly, P.; Dahiya, R. Biodegradable Materials for Sustainable Health Monitoring Devices. *ACS Appl. Bio Mater.* **2021**, *4* (1), 163–194. https://doi.org/10.1021/acsabm.0c01139.

(6) Roth, M. E.; Green, O.; Gnaim, S.; Shabat, D. Dendritic, Oligomeric, and Polymeric Self-Immolative Molecular Amplification. *Chem. Rev.* **2016**, *116* (3), 1309–1352. https://doi.org/10.1021/acs.chemrev.5b00372.

(7) Tan, M. J.; Owh, C.; Chee, P. L.; Kyaw, A. K. K.; Kai, D.; Loh, X. J. Biodegradable Electronics: Cornerstone for Sustainable Electronics and Transient Applications. *J. Mater. Chem. C* **2016**, *4* (24), 5531–5558. https://doi.org/10.1039/c6tc00678g.

(8) Peng, X.; Dong, K.; Wu, Z.; Wang, J.; Wang, Z. L. A Review on Emerging Biodegradable Polymers for Environmentally Benign Transient Electronic Skins. *J. Mater. Sci.* **2021**, *56* (30), 16765–16789. https://doi.org/10.1007/s10853-021-06323-0.

(9) Lu, X. B.; Liu, Y.; Zhou, H. Learning Nature: Recyclable Monomers and Polymers. *Chem. - A Eur. J.* **2018**, *24* (44), 11255–11266. https://doi.org/10.1002/chem.201704461.

(10) Hong, M.; Chen, E. Y. X. Chemically Recyclable Polymers: A Circular Economy Approach to Sustainability. *Green Chem.* **2017**, *19* (16), 3692–3706. https://doi.org/10.1039/c7gc01496a.

(11) Kenley, R. A.; Manser, G. E. Degradable Polymers. Incorporating a Difunctional Azo Compound into a Polymer Network To Produce Thermally Degradable Polyurethanes. *Macromolecules* **1985**, *18* (2), 127–131. https://doi.org/10.1021/ma00144a002.

(12) Ayer, M. A.; Schrettl, S.; Balog, S.; Simon, Y. C.; Weder, C. Light-Responsive Azo-Containing Organogels. *Soft Matter* **2017**, *13* (22), 4017–4023. https://doi.org/10.1039/c7sm00601b.

(13) Mutlu, H.; Geiselhart, C. M.; Barner-Kowollik, C. Untapped Potential for Debonding on Demand: The Wonderful World of Azo-Compounds. *Mater. Horizons* **2018**, *5* (2), 162–183. https://doi.org/10.1039/c7mh00920h.

(14) Feist, J. D.; Lee, D. C.; Xia, Y. A Versatile Approach for the Synthesis of Degradable Polymers via

Controlled Ring-Opening Metathesis Copolymerization. *Nat. Chem.* **2022**, *14* (1), 53–58. https://doi.org/10.1038/s41557-021-00810-2.

(15) Paulusse, J. M. J.; Amir, R. J.; Evans, R. A.; Hawker, C. J. Free Radical Polymers with Tunable and Selective Bio- and Chemical Degradability. *J. Am. Chem. Soc.* **2009**, *131* (28), 9805–9812. https://doi.org/10.1021/ja903245p.

(16) Tachibana, Y.; Baba, T.; Kasuya, K. ichi. Environmental Biodegradation Control of Polymers by Cleavage of Disulfide Bonds. *Polym. Degrad. Stab.* **2017**, *137*, 67–74. https://doi.org/10.1016/j.polymdegradstab.2017.01.003.

(17) Xia, J.; Li, T.; Lu, C.; Xu, H. Selenium-Containing Polymers: Perspectives toward Diverse Applications in Both Adaptive and Biomedical Materials. *Macromolecules* **2018**, *51* (19), 7435–7455. https://doi.org/10.1021/acs.macromol.8b01597.

(18) Kricheldorf, H. R. Syntheses of Biodegradable and Biocompatible Polymers by Means of Bismuth Catalysts. *Chem. Rev.* **2009**, *109* (11), 5579–5594. https://doi.org/10.1021/cr900029e.

(19) Paramonov, S. E.; Bachelder, E. M.; Beaudette, T. T.; Standley, S. M.; Lee, C. C.; Dashe, J.; Fréchet, J. M. J. Fully Acid-Degradable Biocompatible Polyacetal Microparticles for Drug Delivery. *Bioconjug. Chem.* **2008**, *19* (4), 911–919. https://doi.org/10.1021/bc7004472.

(20) Shelef, O.; Gnaim, S.; Shabat, D. Self-Immolative Polymers: An Emerging Class of Degradable Materials with Distinct Disassembly Profiles. *J. Am. Chem. Soc.* **2021**, *143* (50), 21177–21188. https://doi.org/10.1021/jacs.1c11410.

(21) Liang, Y.; Sun, H.; Cao, W.; Thompson, M. P.; Gianneschi, N. C. Degradable Polyphosphoramidate via Ring-Opening Metathesis Polymerization. *ACS Macro Lett.* **2020**, *9* (10), 1417–1422. https://doi.org/10.1021/acsmacrolett.0c00401.

(22) Song, C. C.; Du, F. S.; Li, Z. C. Oxidation-Responsive Polymers for Biomedical Applications. *J. Mater. Chem. B* **2014**, *2* (22), 3413–3426. https://doi.org/10.1039/c3tb21725f.

(23) Wang, L.; Zhu, K.; Cao, W.; Sun, C.; Lu, C.; Xu, H. ROS-Triggered Degradation of Selenide-Containing Polymers Based on Selenoxide Elimination. *Polym. Chem.* **2019**, *10* (16), 2039–2046. https://doi.org/10.1039/c9py00171a.

(24) Miller, K. A.; Morado, E. G.; Samanta, S. R.; Walker, B. A.; Nelson, A. Z.; Sen, S.; Tran, D. T.; Whitaker, D. J.; Ewoldt, R. H.; Braun, P. V.; et al. Acid-Triggered, Acid-Generating, and Self-Amplifying Degradable Polymers. *J. Am. Chem. Soc.* **2019**, *141* (7), 2838–2842. https://doi.org/10.1021/jacs.8b07705.

(25) Xu, Y.; Sen, S.; Wu, Q.; Zhong, X.; Ewoldt, R. H.; Zimmerman, S. C. Base-Triggered Self-Amplifying Degradable Polyurethanes with the Ability to Translate Local Stimulation to Continuous Long-Range Degradation. *Chem. Sci.* **2020**, *11* (12), 3326–3331. https://doi.org/10.1039/c9sc06582b.

(26) Peterson, G. I.; Church, D. C.; Yakelis, N. A.; Boydston, A. J. 1,2-Oxazine Linker As a Thermal Trigger for Self-Immolative Polymers. *Polymer (Guildf).* **2014**, *55* (23), 5980–5985. https://doi.org/10.1016/j.polymer.2014.09.048.

(27) Kiel, G. R.; Lundberg, D. J.; Prince, E.; Husted, K. E. L.; Johnson, A. M.; Lensch, V.; Li, S.; Shieh, P.; Johnson, J. A. Cleavable Comonomers for Chemically Recyclable Polystyrene: A General Approach to Vinyl Polymer Circularity. *J. Am. Chem. Soc.* **2022**, *144* (28), 12979−12988. https://doi.org/10.1021/jacs.2c05374.

(28) Lin, Y.; Kouznetsova, T. B.; Craig, S. L. Mechanically Gated Degradable Polymers. *J. Am. Chem. Soc.* **2020**, *142* (5), 2105–2109. https://doi.org/10.1021/jacs.9b13359.

(29) Parrott, M. C.; Luft, J. C.; Byrne, J. D.; Fain, J. H.; Napier, M. E.; Desimone, J. M. Tunable Bifunctional Silyl Ether Cross-Linkers for the Design of Acid-Sensitive Biomaterials. *J. Am. Chem. Soc.* **2010**, *132* (50), 17928–17932. https://doi.org/10.1021/ja108568g.

(30) Szychowski, J.; Mahdavi, A.; Hodas, J. J. L.; Bagert, J. D.; Ngo, J. T.; Landgraf, P.; Dieterich, D. C.; Schuman, E. M.; Tirrell, D. A. Cleavable Biotin Probes for Labeling of Biomolecules via Azide-Alkyne Cycloaddition. *J. Am. Chem. Soc.* **2010**, *132* (51), 18351–18360. https://doi.org/10.1021/ja1083909.

(31) Bunton, C. M.; Bassampour, Z. M.; Boothby, J. M.; Smith, A. N.; Rose, J. V.; Nguyen, D. M.; Ware, T. H.; Csaky, K. G.; Lippert, A. R.; Tsarevsky, N. V.; et al. Degradable Silyl Ether-Containing Networks from Trifunctional Thiols and Acrylates. *Macromolecules* **2020**, *53* (22), 9890–9900. https://doi.org/10.1021/acs.macromol.0c01967.

(32) Parrott, M. C.; Finniss, M.; Luft, J. C.; Pandya, A.; Gullapalli, A.; Napier, M. E.; Desimone, J. M. Incorporation and Controlled Release of Silyl Ether Prodrugs from PRINT Nanoparticles. *J. Am. Chem. Soc.* **2012**, *134* (18), 7978–7982. https://doi.org/10.1021/ja301710z.

(33) Ware, T.; Jennings, A. R.; Bassampour, Z. S.; Simon, D.; Son, D. Y.; Voit, W. Degradable, Silyl Ether Thiol-Ene Networks. *RSC Adv.* **2014**, *4* (75), 39991–40002. https://doi.org/10.1039/c4ra06997h.

(34) Zhang, S.; Xu, X. Q.; Liao, S.; Pan, Q.; Ma, X.; Wang, Y. Controllable Degradation of Polyurethane Thermosets with Silaketal Linkages in Response to Weak Acid. *ACS Macro Lett.* **2022**, *11* (7), 868–874. https://doi.org/10.1021/acsmacrolett.2c00204.

(35) Husted, K. E. L.; Brown, C. M.; Shieh, P.; Kevlishvili, I.; Kristufek, S. L.; Zafar, H.; Accardo, J. V.; Cooper, J. C.; Klausen, R. S.; Kulik, H. J.; et al. Remolding and Deconstruction of Industrial Thermosets via Carboxylic Acid-Catalyzed Bifunctional Silyl Ether Exchange. *J. Am. Chem. Soc.* **2023**, *145* (3), 1916–1923. https://doi.org/10.1021/jacs.2c11858.

(36) Husted, K. E. L.; Shieh, P.; Lundberg, D. J.; Kristufek, S. L.; Johnson, J. A. Molecularly Designed Additives for Chemically Deconstructable Thermosets without Compromised Thermomechanical Properties. *ACS Macro Lett.* **2021**, *10* (7), 805–810. https://doi.org/10.1021/acsmacrolett.1c00255.

(37) Shieh, P.; Zhang, W.; Husted, K. E. L.; Kristufek, S. L.; Xiong, B.; Lundberg, D. J.; Lem, J.; Veysset, D.; Sun, Y.; Nelson, K. A.; et al. Cleavable Comonomers Enable Degradable, Recyclable Thermoset Plastics. *Nature* **2020**, *583* (7817), 542–547. https://doi.org/10.1038/s41586-020-2495-2.

(38) AlFaraj, Y.; Mohapatra, S.; Shieh, P.; Husted, K.; Ivanoff, D.; Lloyd, E.; Cooper, J.; Dai, Y.; Singhal, A.; Moore, J.; et al. A Model Ensemble Approach Enables Data-Driven Property Prediction for Chemically

Deconstructable Thermosets in the Low Data Regime. **2023**, 1–19.

(39) Shieh, P.; Nguyen, H. V. T.; Johnson, J. A. Tailored Silyl Ether Monomers Enable Backbone-Degradable Polynorbornene-Based Linear, Bottlebrush and Star Copolymers through ROMP. *Nat. Chem.* **2019**, *11* (12), 1124–1132. https://doi.org/10.1038/s41557-019-0352-4.

(40) Johnson, A. M.; Husted, K. E. L.; Kilgallon, L. J.; Johnson, J. A. Orthogonally Deconstructable and Depolymerizable Polysilylethers via Entropy-Driven Ring-Opening Metathesis Polymerization. *Chem. Commun.* **2022**, *58* (61), 8496–8499. https://doi.org/10.1039/d2cc02718f.

(41) Lloyd, E. M.; Cooper, J. C.; Shieh, P.; Ivanoff, D. G.; Parikh, N. A.; Mejia, E. B.; Husted, K. E. L.; Costa, L. C.; Sottos, N. R.; Johnson, J. A.; et al. Efficient Manufacture, Deconstruction, and Upcycling of High-Performance Thermosets and Composites. *ACS Appl. Eng. Mater.* **2023**, *1* (1), 477–485. https://doi.org/10.1021/acsaenm.2c00115.

(42) Smith, R. A.; Fu, G.; McAteer, O.; Xu, M.; Gutekunst, W. R. Radical Approach to Thioester-Containing Polymers. *J. Am. Chem. Soc.* **2019**, *141* (4), 1446–1451. https://doi.org/10.1021/jacs.8b12154.

(43) Prebihalo, E. A.; Luke, A. M.; Reddi, Y.; LaSalle, C. J.; Shah, V. M.; Cramer, C. J.; Reineke, T. M. Radical Ring-Opening Polymerization of Sustainably-Derived Thionoisochromanone. *Chem. Sci.* **2023**, 5689–5698. https://doi.org/10.1039/d2sc06040j.

(44) Delaittre, G.; Barner, L. The Para-Fluoro-Thiol Reaction as an Efficient Tool in Polymer Chemistry. *Polym. Chem.* **2018**, *9* (20), 2679–2684. https://doi.org/10.1039/c8py00287h.

(45) Zhu, P.; Meng, W.; Huang, Y. Synthesis and Antibiofouling Properties of Crosslinkable Copolymers Grafted with Fluorinated Aromatic Side Chains. *RSC Adv.* **2017**, *7* (6), 3179–3189. https://doi.org/10.1039/C6RA26409C.

(46) Ott, C.; Hoogenboom, R.; Schubert, U. S. Post-Modification of Poly(Pentafluorostyrene): A Versatile "Click" Method to Create Well-Defined Multifunctional Graft Copolymers. *Chem. Commun.* **2008**, No. 30, 3516–3518. https://doi.org/10.1039/b807152g.

(47) Atanasov, V.; Kerres, J. Highly Phosphonated Polypentafluorostyrene. *Macromolecules* **2011**, *44* (16), 6416–6423. https://doi.org/10.1021/ma2011574.

(48) Noy, J. M.; Friedrich, A. K.; Batten, K.; Bhebhe, M. N.; Busatto, N.; Batchelor, R. R.; Kristanti, A.; Pei, Y.; Roth, P. J. Para-Fluoro Postpolymerization Chemistry of Poly(Pentafluorobenzyl Methacrylate): Modification with Amines, Thiols, and Carbonylthiolates. *Macromolecules* **2017**, *50* (18), 7028–7040. https://doi.org/10.1021/acs.macromol.7b01603.

(49) Boufflet, P.; Casey, A.; Xia, Y.; Stavrinou, P. N.; Heeney, M. Pentafluorobenzene End-Group as a Versatile Handle for Para Fluoro "Click" Functionalization of Polythiophenes. *Chem. Sci.* **2017**, *8* (3), 2215–2225. https://doi.org/10.1039/c6sc04427a.

(50) Agar, S.; Baysak, E.; Hizal, G.; Tunca, U.; Durmaz, H. An Emerging Post-Polymerization Modification Technique: The Promise of Thiol-Para-Fluoro Click Reaction. *J. Polym. Sci. Part A Polym. Chem.* **2018**, *56* (12), 1181–1198. https://doi.org/10.1002/pola.29004.

(51) Pei, Y.; Noy, J. M.; Roth, P. J.; Lowe, A. B. Thiol-Reactive Passerini-Methacrylates and Polymorphic Surface Functional Soft Matter Nanoparticles via Ethanolic RAFT Dispersion Polymerization and Post-Synthesis Modification. *Polym. Chem.* **2015**, *6* (11), 1928–1931. https://doi.org/10.1039/c4py01558d.

(52) Noy, J. M.; Koldevitz, M.; Roth, P. J. Thiol-Reactive Functional Poly(Meth)Acrylates: Multicomponent Monomer Synthesis, RAFT (Co)Polymerization and Highly Efficient Thiol-Para-Fluoro Postpolymerization Modification. *Polym. Chem.* **2015**, *6* (3), 436–447. https://doi.org/10.1039/c4py01238k.

(53) Gudipati, C. S.; Creenlief, C. M.; Johnson, J. A.; Prayoncpan, P.; Wooley, K. L. Hyperbranched Fluoropolymer and Linear Poly(Ethylene Glycol) Based Amphiphilic Crosslinked Networks as Efficient Antifouling Coatings: An Insight into the Surface Compositions, Topographies, and Morphologies. *J. Polym. Sci. Part A Polym. Chem.* **2004**, *42* (24), 6193–6208. https://doi.org/10.1002/pola.20466.

(54) Gan, D.; Mueller, A.; Wooley, K. L. Amphiphilic and Hydrophobic Surface Patterns Generated from Hyperbranched Fluoropolymer/Linear Polymer Networks: Minimally Adhesive Coatings via the Crosslinking of Hyperbranched Fluoropolymers. *J. Polym. Sci. Part A Polym. Chem.* **2003**, *41* (22), 3531–3540. https://doi.org/10.1002/pola.10968.

(55) Blackmore, P. M.; Feast, W. J. Stereoregular Fluoropolymers: 6. The Ring-Opening Polymerization of N-Pentafluorophenylbicyclo[2.2.1]Hept-5-Ene-2,3-Dicarboximide. *J. Fluor. Chem.* **1988**, *40* (2–3), 331–347. https://doi.org/10.1016/S0022-1139(00)83072-9.

(56) Santiago, A. A.; Vargas, J.; Fomine, S.; Gavino, R.; Tlenkopatchev, M. A. Polynorbornene with Pentafluorophenyl Imide Side Chain Groups: Synthesis and Sulfonation. *J. Polym. Sci. Part A Polym. Chem.* **2010**, *48*, 2925–2933. https://doi.org/10.1002/pola.

(57) Xia, Y.; Li, Y.; Burts, A. O.; Ottaviani, M. F.; Tirrell, D. A.; Johnson, J. A.; Turro, N. J.; Grubbs, R. H. EPR Study of Spin Labeled Brush Polymers in Organic Solvents. *J. Am. Chem. Soc.* **2011**, *133* (49), 19953–19959. https://doi.org/10.1021/ja2085349.

(58) Nguyen, H. V. T.; Detappe, A.; Gallagher, N. M.; Zhang, H.; Harvey, P.; Yan, C.; Mathieu, C.; Golder, M. R.; Jiang, Y.; Ottaviani, M. F.; et al. Triply Loaded Nitroxide Brush-Arm Star Polymers Enable Metal-Free Millimetric Tumor Detection by Magnetic Resonance Imaging. *ACS Nano* **2018**, *12* (11), 11343–11354. https://doi.org/10.1021/acsnano.8b06160.

(59) Golder, M. R.; Liu, J.; Andersen, J. N.; Shipitsin, M. V.; Vohidov, F.; Nguyen, H. V. T.; Ehrlich, D. C.; Huh, S. J.; Vangamudi, B.; Economides, K. D.; et al. Reduction of Liver Fibrosis by Rationally Designed Macromolecular Telmisartan Prodrugs. *Nat. Biomed. Eng.* **2018**, *2* (11), 822–830. https://doi.org/10.1038/s41551-018-0279-x.

(60) Vohidov, F.; Andersen, J. N.; Economides, K. D.; Shipitsin, M. V.; Burenkova, O.; Ackley, J. C.; Vangamudi, B.; Nguyen, H. V. T.; Gallagher, N. M.; Shieh, P.; et al. Design of BET Inhibitor Bottlebrush Prodrugs with Superior Efficacy and Devoid of Systemic Toxicities. *J. Am. Chem. Soc.* **2021**, *143* (12), 4714–4724. https://doi.org/10.1021/jacs.1c00312.

(61) Detappe, A.; Nguyen, H. V. T.; Jiang, Y.; Agius, M. P.; Wang, W.; Mathieu, C.; Su, N. K.; Kristufek, S. L.;

Lundberg, D. J.; Bhagchandani, S.; et al. Molecular Bottlebrush Prodrugs as Mono- and Triplex Combination Therapies for Multiple Myeloma. *Nat. Nanotechnol.* **2023**, *18* (2), 184–192. https://doi.org/10.1038/s41565-022-01310-1.

(62) Bhagchandani, S. H.; Vohidov, F.; Milling, L. E.; Tong, E. Y.; Brown, C. M.; Ramseier, M. L.; Liu, B.; Fessenden, T. B.; Nguyen, H. V. T.; Kiel, G. R.; et al. Engineering Kinetics of TLR7/8 Agonist Release from Bottlebrush Prodrugs Enables Tumor-Focused Immune Stimulation. *Sci. Adv.* **2023**, *9* (16), eadg2239. https://doi.org/10.1126/sciadv.adg2239.

(63) Turgut, H.; Schmidt, A. C.; Wadhwani, P.; Welle, A.; Müller, R.; Delaittre, G. The Para-Fluoro-Thiol Ligation in Water. *Polym. Chem.* **2017**, *8* (8), 1288–1293. https://doi.org/10.1039/c6py02108e.

(64) Serjeant, E. P.; Dempsey, B. *Ionisation Constants of Organic Acids in Aqueous Solution*, IUPAC chem.; Permgamon Press, Inc.: New York, 1979.

(65) Kovačič, S.; Slugovc, C. Ring-Opening Metathesis Polymerisation Derived Poly(Dicyclopentadiene) Based Materials. *Mater. Chem. Front.* **2020**, *4* (8), 2235–2255. https://doi.org/10.1039/d0qm00296h.

Table of contents figure